Chinese Science Bulletin

Amphiphilic dextran/magnetite nanocomposites as magnetic resonance imaging probes

WANG QiaoYing[1*], SU HongYing[1*], XIA ChunChao[2], SUN JiaYu[2], LIU Chen[1], WANG ZhiYong[1], GONG QiYong[2], SONG Bin[2], GAO FaBao[2], AI Hua[1,2†] & GU ZhongWei[1]

[1] National Engineering Research Center for Biomaterials, Sichuan University, Chengdu 610064, China;
[2] Department of Radiology, West China Hospital, Sichuan University, Chengdu 610041, China

Superparamagnetic iron oxide (SPIO) nanoparticles are effective contrast agents for enhancement of magnetic resonance imaging at the tissue, cellular or even molecular levels. High quality SPIO nanoparticles can be synthesized in the organic phase but need to be transferred into water before any biomedical applications. In this study, amphiphilic poly(ε-caprolactone) grafted dextran (Dex-*g*-PCL) was used as carriers for particle encapsulation and stabilization in the aqueous phase. Multiple SPIO nanoparticles were self-assembled together with the help of Dex-*g*-PCL during phase transfer from chloroform to water, and diameters of Dex-*g*-PCL/SPIO nanocomposites were (64 ± 22) nm through dynamic light scattering measurement. These nanocomposites were superparamagnetic at 300 K with saturated magnetization of 88 emu/g Fe. In the magnetic field of 1.5 T, Dex-*g*-PCL/SPIO nanocomposites had a *T*2 relaxivity of 363 Fe mL · mol^{-1} · s^{-1}. This unique nanocomposite brought significant mouse liver contrast with signal intensity changes of –60% at 5 min after intravenous administration. However, uptake of Dex-*g*-PCL/SPIO nanocomposites in liver reticuloendothelial cells (Kupffer cells) did not immediately happen at shorter time points (<4 h) as verified by histology studies, and it was evident that more iron staining would be located in Kupffer cells 24 h after contrast agent administration. After 24 h and 10 d, the signal intensities (SI) gradually recovered, and SI changes were –44% and –31%, respectively. From our observation, the time window for enhanced-MRI could last at least 12 days and totally recovered after 16 days. This novel sensitive MRI contrast agent may find potential applications in discovering small liver lesions such as early tumor diagnosis.

superparamagnetic iron oxide, dextran, micelle, magnetic resonance imaging, contrast agent

Superparamagnetic iron oxide (SPIO) nanocrystals are widely used not only for electronic applications, but also for biomedical applications including magnetic resonance imaging (MRI), biosensing, thermal therapy of cancers and drug delivery[1–4]. High quality iron oxide nanocrystals are synthesized in the organic phase at high temperatures for better control of particle size and morphology[5–7]. These nanocrystals are well soluble in organic solvents but it is necessary to have them well dispersed in water for any biological application. Besides, there are two important prerequisites to satisfy: first, the water soluble particles need to preserve their magnetic properties after phase transfer; second, the coating materials need to be biocompatible and biodegradable for *in vivo* applications. Different materials have been chosen for nanocrystal phase transfer including small molecule ligands[8,9] and poly(ethylene glycol) (PEG)-phosphine oxide polymer[10]. These water soluble SPIO nanoparticles have shown good imaging contrast effects and bio-

Received November 30, 2008; accepted February 26, 2009
doi: 10.1007/s11434-009-0255-7
†Corresponding author (email: huaai@scu.edu.cn)
*Contributed equally to this work
Supported by the Program for New Century Excellent Talents in University (Grant No. NCET-06-0781), Distinguished Young Scholars Project of Sichuan Province (Grant No. 06ZQ026-007), National Natural Science Foundation of China (Grant Nos. 30570514, 50603015 & 50830107) and National Basic Research Program of China (Grant No. 2005CB623903)

Citation: Wang Q Y, Su H Y, Xia C C, et al. Amphiphilic dextran/magnetite nanocomposites as magnetic resonance imaging probes. Chinese Sci Bull, 2009, 54: 2925—2933, doi: 10.1007/s11434-009-0255-7

compatibility. However, the searching of high quality polymer/SPIO nanocomposites as sensitive MRI contrast agents has never stopped.

Polymeric micelles are potential candidates for contrast agent applications. They are nanoscopic core-shell structures self-assembled by amphiphilic block copolymers in aqueous phase[11,12]. They have shown various advantages such as low critical micellar concentration (CMC), reduction in toxic side effects of drugs and long blood circulation time etc., and have long been used for hydrophobic anti-cancer drug encapsulation[13−16]. Not limited to small molecule drugs, the application has been extended to encapsulation of functional nanoparticles including magnetite[14,17] and quantum dots[18,19] for bioimaging. These nanocomposites not only preserve the magnetic and optical properties of the original particles but also show good biocompatibility both *in vitro* and *in vivo*. Particularly, multiple magnetic nanoparticles can be encapsulated inside the hydrophobic core of one micelle, forming a closed packing structure-clustering, which resulted in much stronger T_2 effects than single particle containing micelles at the same iron concentration[17]. This unique structure provides opportunities for design and development of ultrasensitive MR probes.

Polysaccharides are natural polymers usually having good biocompatibility. Dextran, hyaluronic acid, chondroitin sulfate and chitosan have been widely used for drug and gene delivery. Dextran have long been used as a temporary plasma substitute with good biosafety, and also chosen as the material coated on the clinically approved SPIO contrast agents such as Feridex and Resovist. However, dextran itself as a hydrophilic polymer can not be used to stabilize hydrophobic SPIO nanoparticles in water.

In this study, we use amphiphilic dextran as carriers to form polymer/SPIO nanocomposites. We chose poly(ε-caprolactone) (PCL) as the hydrophobic segment and grafted it onto dextran, the main polymer chain. PCL-grafted dextran (Dex-*g*-PCL) was synthesized by ring opening polymerization (ROP) of ε-caprolactone initiated by the free hydroxyl groups (−OH) of silylated dextran. Multiple hydrophobic SPIO nanoparticles stayed inside the Dex-*g*-PCL micelles after phase transfer. The physical properties of composite micelles were characterized through dynamic light scattering, magnetization and T_2 relaxivity. Their MRI contrast effect was tested *in vivo* on mice through liver imaging, and histology slides were prepared to examine the contrast agent uptake by liver at different time points after i.v. injection.

1 Materials and methods

1.1 Materials

Dextran T10 (Mw 10300; Mn 5900) was purchased from Pharmacia and dried under a reduced pressure at 90℃ overnight and then underwent azeotropic distillations with dry pyridine for three times. 1,1,1,3,3,3-Hexamethyldisilazane (HMDS) (Kelong Chemicals) was used after distillation under a reduced pressure. Chlorotrimethylsilane (TMSCl) (99%) was purchased from Sigma and used as received. Stannous octoate ($Sn(Oct)_2$) was purchased from Fluka and used as received. ε-Caprolactone (CL) from Fluka was dried over CaH_2 for 48 h, distilled under reduced pressure, and stored under inert atmosphere. Toluene was dried by refluxing over Na just before use. Dimethyl sulfoxide (DMSO) was dried over CaH_2 and distilled under reduced pressure.

Iron(III) acetylacetonate, 1,2-hexadecanediol (97%), benzyl ether (99%), oleic acid (90%), and oleylamine (>70%) were purchased from Aldrich Chemical Co. and used as received.

1.2 Synthesis of superparamagnetic iron oxide (SPIO) nanocrystals

Detailed synthetic method for SPIO nanocrystals was described in a previous publication by Sun et al[7]. Briefly, $Fe(acac)_3$ (1 mmol) was mixed with 1,2-hexadecanediol (5 mmol), oleic acid (3 mmol), and oleylamine (3 mmol) in benzyl ether (10 mL) under argon protection. The mixture was then heated to reflux (300℃) for 1 h. After cooling to room temperature, the solution was treated with ethanol to yield a dark-brown precipitate. The product was redispersed in hexane in the presence of oleic acid and oleylamine and reprecipitated with ethanol. Finally, these nanocrystals were dispersed in hexane for storage.

1.3 Dextran silylation

The synthetic process of Dex-*g*-PCL is illustrated in Scheme 1; it includes dextran silylation, ROP of CL from silylated dextran, and deprotection of the silylated Dex-*g*-PCL. First, dextran silylation was carried out according to a recent publication[20]. An amount of 0.25 g

dry dextran was totally dissolved in 10 mL DMSO in a previously dried two-neck flask, and desired amounts of HMDS and TMSCl were added under an argon flow with dried syringes. After 4 h of reaction, 4 mL of dry toluene was added into the medium to make the reaction condition homogeneous during silylation. The reaction system was kept at 50℃ for 20 h. The expected silylated dextran was recovered by precipitation from cooled heptane, dried in a vacuum. Protection yield (silylation yield) of as-prepared silylated dextran was calculated by ^{1}H NMR in $CDCl_3$ as described earlier using eq.(1)[21].

$$\text{Yield}\,(\%)=\frac{A_{\text{OSiMe}_3}}{A_{\text{glucosidicH}}}\frac{6\times100}{27}, \tag{1}$$

where A_{OSiMe_3} and $A_{\text{glucosidicH}}$ are the respective integral intensities of trimethylsilyl group at 0.15 ppm (1 ppm = 10^{-6}) and glucosidic proton from 3.0 to 4.0 ppm. The degree of substitution was calculated as eq. (2):

$$DS=\frac{3\text{Yield}\,(\%)}{100}. \tag{2}$$

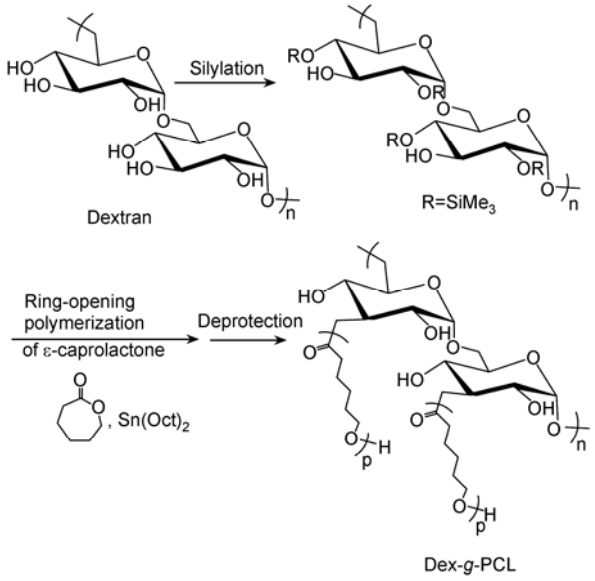

Scheme 1 The synthetic process of poly(ε-caprolactone)-grafted dextran.

1.4 ROP of CL from silylated dextran

In a typical experiment, the synthesis of Dex-*g*-PCL was performed by the ROP of CL in the presence of $Sn(Oct)_2$. The polymerization was carried out in dry toluene under Ar at 105℃ for 48 h according to a recent publication[22]. Silylated dextran was dissolved in dry toluene (10 wt% silylated dextran) after azeotropic distillations with dry toluene for three times, then desired amount of CL was secondly added, and a trace amount of $Sn(Oct)_2$ was added after the reaction system became clear. The expected product was recovered by precipitation in cool heptane.

PCL weight fraction in TMSD-*g*-PCL copolymers (F_{PCL}) was determined by ^{1}H NMR spectroscopy as follows[22]:

$$\begin{aligned}F_{\text{PCL}}=I_{\text{PCL}}MW_{\text{CL}}\Big/\Big\{&\left(I_{\text{PCL}}MW_{\text{CL}}\right)\\&+\left(\left(I_{\text{dextran}}/3\right)\Big[MW_{\text{GL}}+\left(DS\times MW_{\text{"SiMe}_3\text{"}}\right)\right.\\&\left.+\left[(3-DS)\times MW_{\text{"H"}}\right]\Big]\right)\Big\},\end{aligned} \tag{3}$$

where I_{PCL} was the average value of ^{1}H NMR integral intensity obtained from the methylene protons at 4.00 ppm ("—C**H**$_2$—O—C(O) —") and 2.27 ppm ("—O—C(O)—C**H**$_2$—"), I_{dextran} was ^{1}H NMR integral intensity of glucosidic proton from 3.0 to 4.0 ppm; DS was degree of substitution by silylation; MW_{CL}, $MW_{\text{"SiMe}_3\text{"}}$, $MW_{\text{"H"}}$, and MW_{GL} are 114.1, 73.2, 1.0, and 159.1 respectively. MW_{GL} corresponds actually to one $C_6H_7O_5$ "deprotonated" glucosidic unit.

1.5 Deprotection of the silylated dextran-*g*-PCL

The as-prepared silylated Dex-*g*-PCL was dispersed in dioxane containing 0.1 M HCl. After stirring at room temperature for 2 h, the deprotected copolymers were recovered by precipitation in cool heptane and dried in vacuum.

1.6 Characterization of dextran and amphiphilic dextran

^{1}H NMR spectra were recorded using a Bruker AM 400 apparatus (400 MHz) in d_6-DMSO, $CDCl_3$ using tetramethylsilane (TMS) as an internal reference, or D_2O at 25℃. FT-IR spectra were recorded using a Perkin-Elmer Spectrum One FTIR spectrometer.

1.7 Preparation of Dex-*g*-PCL/SPIO nanocomposites

The Dex-*g*-PCL/SPIO nanocomposites were produced according to an emulsion and solvent evaporation method[17] with minor modification. Briefly, appropriate amount of copolymer and SPIO nanoparticles (polymer/SPIO mass ratio = 3) were dissolved in 0.5 mL chloroform and added into 5 mL Milli-Q water under probe sonication (SONICS, US), Dex-*g*-PCL/SPIO nanocomposites in water were obtained after evaporation of chloroform. Particle size distributions were

characterized through dynamic light scattering (DLS) measurement using a Malvern Nanosizer.

1.8 Magnetization and T_2 relaxivity studies

Elemental analysis of iron from Dex-*g*-PCL/SPIO nanocomposite samples was performed using an atomic absorption spectroscopy (AAS) (AA800, Perkin-Elmer, USA). Magnetic studies were carried out using a MPMS7 Quantum Design SQUID magnetometer (Quantum Design, San Diego, USA) at 300 K. Sample in aqueous phase was lyophilized and then measured with a scope of −10—10 kOe, 4 quadrants. T_2 relaxivities were measured at 1.5 T on a clinical MR scanner (Siemens Sonata) at room temperature as described before[17]. The T_2-weighted images were acquired with a conventional spin echo acquisition (TR = 5000 ms) with TE values ranging from 6 to 170 ms. Relaxivity values of r_2 were calculated through the curve fitting of $1/T_2$ relaxation time (s^{-1}) vs. the iron concentration (mM).

1.9 *In vivo* MRI studies

All studies involving animals were approved by the Animal Care and Use Committee of the Institute. MRI studies were performed with a 3 T imaging system (Philips Medical System) by using a mouse coil (Philips) for transmission and reception of the signal. Multisection T_2-weighted TSE sequence (TR = 1000 ms; TE = 80 ms; FOV 25 mm×25 mm; slice thickness 1.6 mm; flip angle 90°) was used for all our studies. Mice were anaesthetized by pentobarbital sodium at the dose of 40 mg/kg body weight. MRI scan was performed before and at different time points up to 16 days after contrast agent administration at a dose of 2.5 mg Fe/kg body weight. Signal intensity (SI) was measured for each time point and the relative SI changes were plotted against time.

1.10 Histology analysis

Mice were sacrificed at different time points after tail vein injection of Dex-*g*-PCL/SPIO nanocomposites. Liver and spleen tissues were taken out and fixed in 4% buffered paraformaldehyde for more than 48 h, and then embedded in paraffin. Adjacent slides were prepared for histological analysis using either hematoxylin-eosin (HE) staining or Prussian blue staining (iron staining).

2 Results and discussion

2.1 Synthesis of Dex-*g*-PCL

The brush-like amphiphilic graft copolymers were synthesized by a three-step procedure (Scheme 1). The fist step consists of a reversible protection of the hydroxyl groups (—OH) of dextran by using HMDS as silylation agent, followed by the ROP of CL in toluene initiated by remaining —OH groups. The final step involves the removal of trimethylsilyl protecting groups on the dextran backbone. In order to control the amount of PCL grafts and the solubility of trimethylsilyl dextran (TMSD) in organic solvents, protection yields were controlled to be higher than 80%.

The ^{1}H NMR spectra of pure dextran, TMSD-*g*-PCL and Dex-*g*-PCL are shown in Figure 1. Compared with pure dextran (Figure 1(1)), the peaks corresponding to PCL and $OSiMe_3$ can be observed in the spectrum of TMSD-*g*-PCL (Figure 1-(2)): δ (ppm) 1.39 (PCL —$COCH_2$-$CH_2C\mathbf{H}_2CH_2CH_2O$—), 1.66 (PCL —$COCH_2C\mathbf{H}_2CH_2$-$C\mathbf{H}_2CH_2O$—), 2.27 (PCL —$COC\mathbf{H}_2CH_2CH_2CH_2$-$CH_2O$—), 4.00 (PCL —$COCH_2CH_2CH_2CH_2C\mathbf{H}_2O$—), 0.15 (—$OSi(C\mathbf{H}_3)_3$). The protection yield was determined by ^{1}H NMR from the relative intensities of the trimethylsilyl groups at 0.15 ppm and the glucosidic

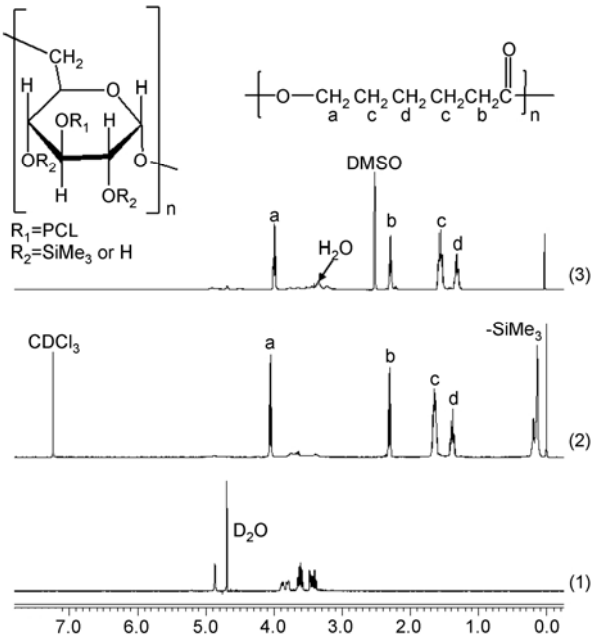

Figure 1 ^{1}H NMR spectra of pure Dextran (1), TMSD-*g*-PCL (2) and Dex-*g*-PCL (3). Solvent = D_2O, $CDCl_3$ and d_6-DMSO at room temperature.

proton centered at 3.0 to 4.0 ppm using $CDCl_3$ as the solvent. The calculated protection yield is 91.5% according to eq. (1) and the DS value is 2.7 as calculated from eq. (2). PCL weight fraction F_{PCL} is about 0.55 as we calculated from eq. (3). The reversible protection of the hydroxyl groups (—OH) with $SiMe_3$ is also demonstrated by the ^1H NMR spectrum (Figures 1(2) & (3)).

Figure 2 shows the FTIR spectra of pure dextran, TMSD and Dex-*g*-PCL. Protection of —OH through silylation is demonstrated by the presentation of absorption bands of the trimethylsilyl groups at 748, 844, 874, 1020, 1164 and 1252 cm^{-1}, and the complete deprotection is also demonstrated by the disappearance of these peaks. Our observation is similar to a previous report[22]. Also, the absorption band at ca. 3500 cm^{-1} of Dex-*g*-PCL resumes to a similar level of pure dextran after deprotection of hydroxyl groups from TMSD-*g*-PCL. Grafting of PCL on dextran is easily evidenced as we can see the absorption peak of C=O from PCL at 1726 cm^{-1} in FTIR spectrum.

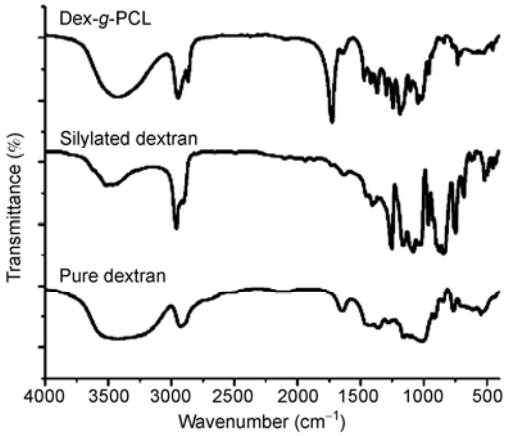

Figure 2 FTIR spectra of pure dextran, silylated dextran and Dex-*g*-PCL.

2.2 Preparation of Dex-*g*-PCL/SPIO nanocomposites

The one-pot reaction led to the monodisperse SPIO nanocrystals that can be easily isolated from the reaction by-products and the ether solvent. Figure 3(a) displays the DLS data of SPIO nanocrystals in hexane with a diameter of (10.1±2.5) nm. In comparison, SPIO nanocrystal containing micelles have a diameter of (64.2±22.2) nm (Figure 3(b)), obviously larger than that of the single SPIO particles in organic solvent. The enlarged particle size is mainly due to amphiphilic dextran coating and multiple particles loading. Under SEM observation, these nanocomposites have even bigger diameters than that in water; probably due to the micelle flatten out after the drying process (Figure 3(c)).

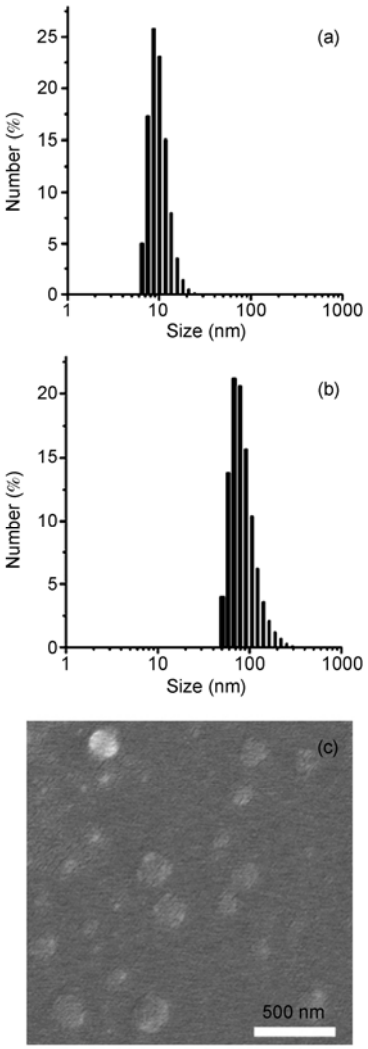

Figure 3 DLS of SPIO nanocrystals in hexane (a) and Dex-*g*-PCL/SPIO nanocomposites in water (b) and SEM images (c) with a scale bar of 500 nm.

2.3 Magnetization and T_2 relaxivity of Dex-*g*-PCL/SPIO nanocomposites

SPIO nanocrystals are superparamagnetic at room temperature with a saturation magnetization about 102 emu/g Fe[23]. Magnetization of the superparamagnetic materials does not vary linearly with the applied field, which is different from that of the paramagnetic colloids[24]. Magnetization measurements of lyophilized sample powder of Dex-*g*-PCL/SPIO nanocomposites show that the net magnetization returned to zero in the absence of an external field, indicating they are superparamagnetic at 300 K (Figure 4). Under a large external

field, the magnetization of the nanocrystals aligns with the field direction and reaches its saturation value (saturation magnetization, σ_s). The σ_s of Dex-*g*-PCL/SPIO micelles slightly reach over 88 emu/g Fe, which is lower than that of single SPIO nanocrystals. The exact reason is still under investigation and similar phenomenon has been discovered before for polymer coated hydrophilic magnetite nanoparticle clusters[25].

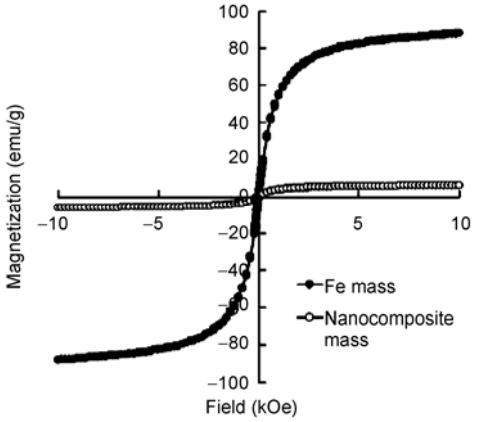

Figure 4 Hysteresis loops of the Dex-*g*-PCL/SPIO nanocomposites containing micelles measured at 300 K. Black dots are plotted based on Fe mass in the composite sample; empty circles represent data based on the total nanocomposite sample mass, which includes mass from Dex-*g*-PCL and SPIO nanoparticles.

To understand how these nanocrystals containing Dex-*g*-PCL micelles function as MRI contrast agents, we studied their relaxivities at 1.5 T field in a clinical MRI scanner. SPIO based MRI contrast agents shorten the T_2 (spin-spin) relaxation times, and their net effectiveness is expressed as T_2 relaxivity (r_2), which represents the reciprocal of the relaxation time per unit concentration of metal ions, with units Fe $mL \cdot mol^{-1} \cdot s^{-1}$. Figure 5(a) displays the T_2 rates of SPIO nanoparticle loaded micelles over iron concentrations. At the magnetic field of 1.5 T, micelles containing multiple SPIO nanocrystals have a reasonably high T_2 relaxivity of 363 Fe $L \cdot mol^{-1} \cdot s^{-1}$. The T_2 relaxivity increased dramatically with SPIO clustering inside micelles, and it is assumed that the enhancement of spin-spin relaxation reflects the ability of magnetic particles to distort the local magnetic field[24]. Larger clusters of SPIO nanocrystals in solution have higher magnetic moments per particle in solution, and distort the magnetic field in larger volumes of solvent. Similar phenomena were found in mPEG-*b*-PCL/SPIO micelles and polyelectrolyte-neutral copolymer/SPIO aggregates[17,26]. Although relaxation theory for single SPIO particles has been developed[27], no quantitative microscopic theory is available to explain the T_2 relaxivity changes for clustered SPIO particles.

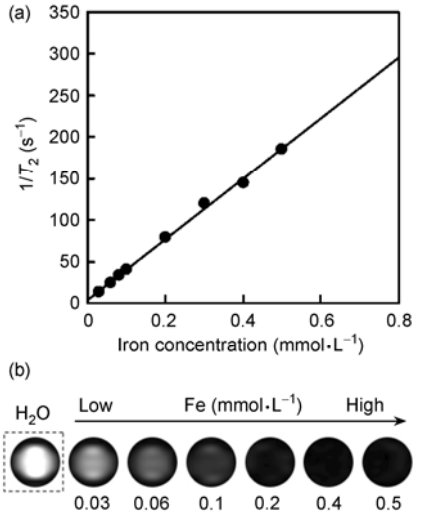

Figure 5 (a) T_2 relaxation rate ($1/T_2$, s^{-1}) as a function of Fe concentration (mM) for SPIO nanocrystal loaded Dex-*g*-PCL micelles at 1.5 T; (b) T_2-weighted MRI images (1.5 T, spin-echo sequence: TR = 5000 ms, TE = 50 ms) of the above micelle formulations.

To quantify MRI detection limit, we define the sensitivity as Dex-*g*-PCL/SPIO nanocomposite concentrations at which MRI signal intensity decreases to 50% of that for pure water in T_2-weighted images (1.5 T, spin-echo sequence: TR = 5000 ms, TE = 35 ms). For multiple SPIO nanoparticles containing micelles, the detection limit is 0.06 mM Fe. The sensitivity of multiple SPIO nanocrystal loaded micelles may prove to be essential in detecting minor pathological changes at molecular or cellular levels.

2.4 *In vivo* MRI study

SPIO contrast agents can enhance the image contrast of tissues through substantial shortening of T_2 relaxation times, leading to hypointense signals at locations where the probes accumulate. For liver imaging, SPIO agents have been extremely useful in diagnosis of small tumor, metastasis, fibrosis, cirrhosis, and other focal lesions[28–30]. The observed effects on signal intensity depend on various factors, including the T_2 relaxivity and pharmacokinetics of the agents, the dose of administration, the type of coils, and the acquisition parameters. The T_2 relaxivity of Dex-*g*-PCL/SPIO nanocomposites is 363 Fe m $L \cdot mol^{-1} \cdot s^{-1}$, much higher than that of the

commercially available contrast agents such as Feridex (98 Fe mL·mol^{-1}·s^{-1}) and Resovist (151 Fe mL·mol^{-1}·s^{-1})[31]. Another important parameter to adjust is the pulse sequence which can be crucial in determining the diagnostic effectiveness of contrast agents. Turbo spin-echo (TSE) and fast gradient-recalled echo (GRE) sequences are the most commonly used ones so far.

In our study, we tested both T_2^*-weighted GRE sequence and T_2-weighted TSE sequence with a mouse coil in preliminary observations, and we found that TSE sequence was more effective in obtaining high quality images. Similar findings were also reported before because T_2^*-weighted GRE sequences are more sensitive to motion artifacts such as breath[30,32], which can compromise image quality. T_2-weighted TSE sequence was chosen for the whole study. To compare the signal intensity changes of liver, we kept sequence parameters TR (1000 ms) and TE (80 ms) unchanged for all animal scans. Liver images were taken before and up to 16 days after contrast agent administration (Figure 6(a)). The darkening of liver tissues is obvious comparing with the brightening of gallbladder from 5 min to other time points after tail vein injection of Dex-*g*-PCL/SPIO nanocomposite solutions.

Average relative liver signal intensities (SI) are plotted at different time points in Figure 6(b). Relative SI change was defined as enhancement (ENH) and was calculated as the difference between SI pre and SI post divided by SI pre multiplied with −100 (ENH [%] = ((SI pre-SI post)/SI pre)*(−100)) according to a previous study[33]. Significant liver contrast enhancement was found immediately (5 min) after injection of composite micelles with about −60% SI change. The mean values of SI recovered to 51%, which was −49% change at 3 hours after injection, and approached to 56% at 24 hours. The liver SI changes gradually decreased with the elapse of time. Finally, the SI returned to the baseline 16 days after administration of SPIO micelles. In comparison, the clinically approved liver contrast agents Feridex and Resovist could also bring significant signal changes in a short time after SPIO injection[30,34]. It was reported that liver SI significantly dropped (ENH: −57.7%) 10 min after injection of Resovist (ferucarbotran), and there were no differences in diagnostic performance with images obtained 10 and 40 min after injection[30,35]. The significant SI changes brought by our formulation may found to be promising in discovering small focal hepatic lesions.

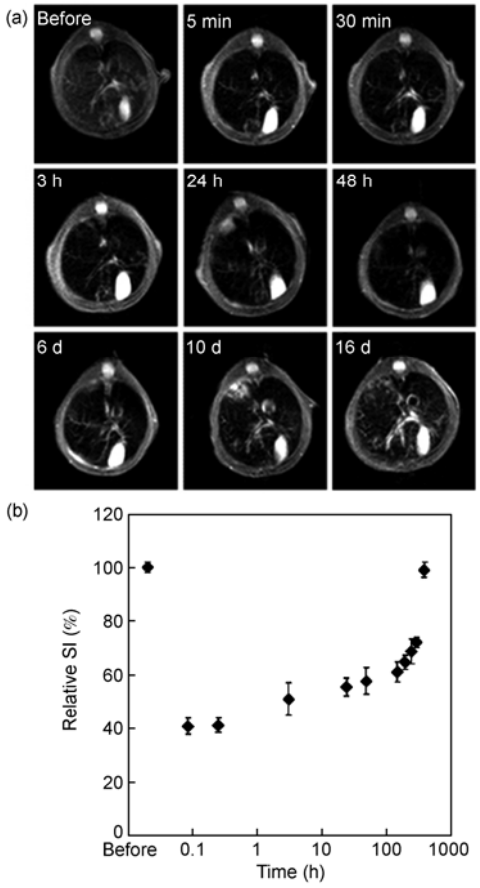

Figure 6 (a) Mouse liver T_2-weighted TSE images at different time points before and after administration of SPIO micelles; (b) mean values of relative SI collected before and after micelle administration.

The time window of Dex-*g*-PCL/SPIO based contrast agents can last up to 12 days with obvious SI changes. Clinical studies have revealed that the time window for Resovist contrast-enhanced MRI of liver is at least 1 day and can reach 4 days on different patients, while Feridex can last up to one week[30]. The imaging contrast of liver brought by SPIO agents have long been believed to be based on RES cell uptake of iron oxide nanoparticles[31]. Many factors influence the pharmacokinetics of the formulation including particle size, surface coating material, surface charge density, etc., thus determining how long particles can circulate in the blood and how they will interact with Kupffer cells. The coating on Feridex is dextran and carboxydextran for Resovist, similar to the coating material of Dex-*g*-PCL/SPIO nanocomposites. For tissue samples obtained within four hours of contrast agent administration, only a few blue dots could be found in Prussian blue stained liver and spleen slides,

suggesting that contrast effect was mainly dependent on the particle distribution in extracellular space including blood. In comparison, more iron staining was discovered for 24 h tissue samples (Figure 7(a)) and they were mostly in Kupffer cells. This means that at longer time points, the contrast enhancement of liver tissues will mainly depend on the RES uptake and some from the extracellular volume. Similar results of RES uptake were reported before for ferumoxtran in rats at the dose of 150 μmol Fe/kg, because RES accumulation of iron peaked between 8 and 24 hours[36]. In spleen slides, Prussian blue stained dots are mostly in red pulp and barely in white pulp (Figure 7(c)), because the macrophages in red pulp has the ability to uptake and remove nanoparticles[37]. The exact iron transport and metabolism mechanism is not clear for this formulation. For carboxydextran or dextran coated iron oxide nanoparticles such as Resovist or Feridex, hydrolytic enzymes were found to degrade intracellular SPIO particles, making the iron lose its crystalline structure and causing a loss of r_2 relaxivity[24].

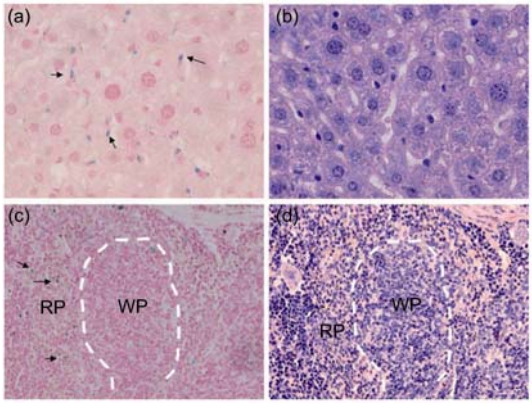

Figure 7 Histology slides of samples 24 hours after contrast agent administration. (a) and (b) Prussian blue and HE histology figures of adjacent liver tissue slides (magnification: 400×); (c) and (d) Prussian blue and HE histology figures of adjacent spleen tissue slides (magnification: 400×). WP = white pulp; RP = red pulp; arrows are pointing to Prussian blue stains.

3 Conclusions

In summary, superparamagnetic iron oxide (SPIO) nanocrystals were synthesized in organic phase and then stabilized in water with the help of PCL-grafted dextran (Dex-*g*-PCL). Multiple SPIO nanoparticles were loaded into Dex-*g*-PCL micelles with mean diameter below 100 nm. This novel formulation was superparamagnetic at room temperature and the T_2 relaxivity reached 363 Fe mL·mol^{-1}s^{-1}, much higher than that of most commercial contrast agents. MRI study *in vivo* indicated that T_2-weighted signal intensity in mouse liver dropped to 40% at 5 minutes after tail vein administration and the time window for enhanced-MRI was at least 12 days. This nanocomposite formulation may prove to be sensitive in discovering small liver lesions.

1 Feng L, Song Y, Wan M, et al. Research progress of magnetic iron oxide nanoparticles. Chin Sci Bull, 2001, 46: 1321－1325
2 Yan G, Zhuo R. Research progress of magnetic resonance imaging contrast agents. Chin Sci Bull, 2001, 46: 1233－1237
3 Bulte J W, Kraitchman D L. Iron oxide MR contrast agents for molecular and cellular imaging. NMR Biomed,2004, 17: 484－499
4 Weissleder R, Mahmood U. Molecular imaging. Radiology, 2001, 219: 316－333
5 Jana N R, Chen Y, Peng X. Size- and shape-controlled magnetic (Cr, Mn, Fe, Co, Ni) oxide nanocrystals via a simple and general approach. Chem Mater, 2004, 16: 3931－3935
6 Park J, An K, Hwang Y, et al. Ultra-large-scale syntheses of monodisperse nanocrystals. Nat Mater, 2004, 3: 891－895
7 Sun S H, Zeng H, Robinson D B, et al. Monodisperse MFe_2O_4 (M = Fe, Co, Mn) nanoparticles. J Am Chem Soc, 2004, 126: 273－279
8 Jun Y W, Huh Y M, Choi J S, et al. Nanoscale size effect of magnetic nanocrystals and their utilization for cancer diagnosis via magnetic resonance imaging. J Am Chem Soc, 2005, 127: 5732－5733
9 Song H T, Choi J S, Huh Y M, et al. Surface modulation of magnetic nanocrystals in the development of highly efficient magnetic resonance probes for intracellular labeling. J Am Chem Soc, 2005, 127: 9992－9993
10 Kim S W, Kim S, Tracy J B, et al. Phosphine oxide polymer for water-soluble nanoparticles. J Am Chem Soc,2005, 127: 4556－4557
11 Kakizawa Y, Kataoka K. Block copolymer micelles for delivery of gene and related compounds. Adv Drug Deliv Rev, 2002, 54: 203－222
12 Kwon G S, Okano T. Polymeric micelles as new drug carriers. Adv Drug Deliv Rev, 1996, 21: 107－116
13 Croy S R, Kwon G S. Polymeric micelles for drug delivery. Curr Pharm Des, 2006, 12: 4669－4684
14 Nasongkla N, Bey E, Ren J, et al. Multifunctional polymeric micelles as cancer-targeted, MRI-ultrasensitive drug delivery systems. Nano Lett, 2006, 6: 2427－2430
15 Nasongkla N, Shuai X, Ai H, et al. cRGD-functionalized polymer micelles for targeted doxorubicin delivery. Angew Chem Int Ed Engl, 2004, 43: 6323－6327
16 Shuai X, Ai H, Nasongkla N, et al. Micellar carriers based on block copolymers of poly(epsilon-caprolactone) and poly(ethylene glycol) for doxorubicin delivery. J Control Release, 2004, 98: 415－426
17 Ai H, Flask C, Weinberg B, et al. Magnetite-loaded polymeric micelles as ultrasensitive magnetic-resonance probes. Adv Mater, 2005, 17: 1949－1952
18 Dubertret B, Skourides P, Norris D J, et al. *In vivo* imaging of quantum dots encapsulated in phospholipid micelles. Science, 2002, 298:

1759－1762

19 Gao X, Cui Y, Levenson R M, et al. *In vivo* cancer targeting and imaging with semiconductor quantum dots. Nat Biotechnol, 2004, 22: 969－976

20 Nouvel C, Dubois P, Dellacherie E, et al. Silylation reaction of dextran: effect of experimental conditions on silylation yield, regioselectivity, and chemical stability of silylated dextrans. Biomacromolecules, 2003, 4: 1443－1450

21 Bajgai M P, Aryal S, Lee D R, et al. Physicochemical characterization of self-assembled poly(epsilon-caprolactone) grafted dextran nanoparticles. Colloid Polym Sci, 2008, 286: 517－524

22 Ydens I, Rutot, D, Degee, P, et al. Controlled synthesis of poly (epsilon-caprolactone)-grafted dextran copolymers as potential environmentally friendly surfactants. Macromolecules, 2000, 33: 6713－6721

23 Xie J, Peng S, Brower, N, et al. One-pot synthesis of monodisperse iron oxide nanoparticles for potential biomedical applications. Pure Appl Chem, 2006, 78: 1003－1014

24 Josephson,L, Lewis J, Jacobs P, et al. The effects of iron oxides on proton relaxivity. Magn Reson Imaging, 1988, 6: 647－653

25 Ditsch A, Laibinis P E, Wang D I C, et al. Controlled clustering and Enhanced tability of olymer-oated agnetic anoparticles. Langmuir, 2005, 21: 6006－6018

26 Berret J F, Schonbeck N, Gazeau F, et al. Controlled clustering of superparamagnetic nanoparticles using block copolymers: Design of new contrast agents for magnetic resonance imaging. J Am Chem Soc, 2006, 128: 1755－1761

27 Koenig S H, Kellar K E. Theory of $1/T_1$ and $1/T_2$ NMRD profiles of solutions of magnetic nanoparticles. Magn Reson Med, 1995, 34: 227－233

28 Aguirre D A, Behling C A, Alpert, E, et al. Liver fibrosis: Noninvasive diagnosis with double contrast material-enhanced MR imaging. Radiology,2006, 239: 425－437

29 Kato N, Ihara S, Tsujimoto T, et al. Effect of resovist on rats with different severities of liver cirrhosis. Invest Radiol, 2002, 37: 292－298

30 Reimer P, Balzer T. Ferucarbotran (Resovist): A new clinically approved RES-specific contrast agent for contrast-enhanced MRI of the liver: Properties, clinical development, and applications. Eur Radiol, 2003, 13: 1266－1276

31 Wang Y X, Hussain S M, Krestin G P. Superparamagnetic iron oxide contrast agents: Physicochemical characteristics and applications in MR imaging. Eur Radiol, 2001, 11: 2319－2331

32 Kim S H, Choi D, Lim H K, et al. Detection of hepatic VX2 carcinomas with ferucarbotran-enhanced magnetic resonance imaging in rabbits: Comparison of nine pulse sequences. Eur J Radiol, 2006, 59: 413－423

33 Reimer P, Muller M, Marx C, et al. Evaluation of the time window for Resovist-enhanced T_2-weighted MRI of the liver. Academic radiology, 2002, 9 (Suppl 2): 336－338

34 Weissleder R, Hahn P F, Stark D D, et al. Superparamagnetic iron oxide: enhanced detection of focal splenic tumors with MR imaging. Radiology, 1998, 169: 399－403

35 Shamsi K, Balzer T, Saini S, et al. Superparamagnetic iron oxide particles (SH U 555 A): Evaluation of efficacy in three doses for hepatic MR imaging. Radiology, 1998, 206: 365－371

36 Van Beers B E, Sempoux C, Materne R, et al. Biodistribution of ultrasmall iron oxide particles in the rat liver. J Magn Reson Imaging, 2001, 13: 594－599

37 Moghimi S M, Hunter A C, Murray J C. Long-circulating and target-specific nanoparticles: theory to practice. Pharmacol Rev, 2001, 53: 283－31